5th African International Conference on Industrial Engineering and Operations Management, Johannesburg/Pretoria, South Africa, April 23 - 25, 2024
Publisher: IEOM Society International, USA
Published: April 23, 2024 DOI: 10.46254/AF05.20240027

Thermodynamic and Sustainability Analysis of a Novel Solar-Powered ORC System Integrated with Single-Effect Absorption-VCP Refrigeration Cycles for Domestic Electricity/Cooling Supply

Fidelis I. Abam
Department of Mechanical Engineering,
University of Calabar,
Nigeria
fidelisabam@unical.edu.ng

Bassey B. Okon
Department of Mechanical Engineering,
Federal University of Technology, Ikot Abasi,
Nigeria
engrbasseyokon@gmail.com

Isuamfon Edem
Department of Mechanical Engineering,
Akwa Ibom State University Ikot Akpaden,
Nigeria
isuamfonedem@yahoo.com

Abstract

Energy is an essential indicator of economic expansion. One way to advance energy needs and environmental sustainability is to develop new, clean, alternative, and possible energy sources. The current study thus proposes a novel power and cooling solar organic Rankine cycle (ORC) with vapour absorption (VAS) and vapour compression refrigeration (VCP) as bottoming cycles. The bottoming cycle uses ammonia–water as the working fluid. In contrast, the topping cycle is driven by ORC based on organic refrigerant. The benefit of the integrated cycle is the production of equivalent refrigerating effects from the two cooling evaporators. The system was analysed using Engineering Equation Solver (EES) Software. The overall efficiencies were calculated at 38.63 and 42.09 % for energy and exergy, respectively, with total evaporating effect, power output, and coefficient of performance estimated at 1358 kW, 26.65 kW and 2.34, in that order. The simulated results showed a 40 % and 55% rise in energy and exergy efficiencies at increased turbine inlet temperatures. Equally, at a higher generator pressure of 4.75 bar, the coefficient of performance reached 3.046. The results indicated an increased energetic sustainability index with increasing generator pressure. Other sustainability indicators, such as waste exergy ratio and environmental effect factors, were found to decrease. The proposed cycle was found to have less environmental impact.

Keywords
Solar-ORC, Ammonia-Water, Exergy, Energy, COP

1. Introduction

Most thermal heat recovery systems applied globally are designed mainly to meet power generation, with little application for cooling and heating production (Ayou and Eveloy 2020). Conversely, several cogeneration or combined power and cooling plants have been proposed extensively by scholars to concurrently meet the electrical power production and cooling demand utilising mid and low-quality thermal energy. Additionally, using binary working fluids with variable condensation and boiling temperatures enhances the overall thermodynamic performance of systems. The latter is ascribed to a good thermal match between the system working medium and the source heat, thus reducing the irreversibility along the flowing heat streams. The use of ammonia with water as a binary combination holds copious benefits. Moreover, because ammonia is comparatively cheap, it has a low environmental effect. Water and ammonia have analogous molecular weights, although the boiling point of ammonia is considerably lesser, making it virtually appropriate to be employed in low-heat temperature systems (Padilla et al. 2010; Kim, 2011). Furthermore, with the universal consumption of fossil fuels and resulting environmental concerns, considerable responsiveness has been drawn to the extension and use of low-grade heat and renewable Energy, comprising solar Energy, waste heat from the industry, and geothermal heat resources (Wang et al. 2016). Among the several utilization methods, the combined power and cooling plants display notable energy transfer effectiveness, making it a promising technology to supply both refrigerating effects and power simultaneously.

2. Theoretical Review

Studies exist vis-à-vis the combined power and cooling cycles based on NH_3-H_2O as a working fluid. The work of Goswami (Goswami, 1995; Goswami, 1998) proposed an innovative combined power cycle for power and cooling production using a single-heat source. The anticipated cycle substituted an NH_3-H_2O turbine system for a condenser plus a throttle valve in the NH_3-H_2O absorption refrigeration system. The study achieved an innovative configuration of an ORC system integrating an absorption refrigeration system. Further investigations by (Goswami and Xu, 1999; Xu et al. 2000) enhanced the anticipated combined cycle, called the Goswami cycle (GOC), by incorporating a superheater in the middle of the turbine and condenser/rectifier to increase the inlet temperature of the turbine, thus enhancing the power output. Yu et al. (2014) examined the thermodynamic performance of the GOC. The results showed that increased turbine inlet pressure decreases system output power. Meanwhile, the specific cooling rate, overall work output, and thermal efficiency maintain the highest values. Nonetheless, the GOC produces a low cooling effect since the turbine exhaust leaves through a thermal heat exchanger (cooler), transmitting merely sensible heat. Some scholars have used NH_3-H_2O working fluid in an adapted Kalina cycle (KC) to achieve a cooling rate by incorporating related components, for instance, the evaporator and valve. Jing et al. (2014) proposed a KC system that interconnected the KC with an NH_3-H_2O absorption refrigeration cycle (ARC) with a pre-cooler, forming a novel power-cooling configuration system with variable power-to-cooling ratios.

Furthermore, (Sun et al. 2013) proposed a unique NH_3-H_2O power-cooling cogeneration cycle using low-temperature heat comprising an ORC and an ARC. The study achieved energy and exergy efficiencies of 40.6 % and 36.4 %, respectively, with a cooling rate of 13 kW. Han et al. (2014) proposed an NH_3-H_2O power-cooling cogeneration cycle that employed the turbine's exhaust vapour. The study obtained a cooling rate of 11.67 kW, with coefficient of performance and conversion efficiency of 0.465 and 3.98 %, respectively. Like Mendoza et al. (2014), other investigators proposed a solo-stage combined absorption power-cooling system with dual refrigeration and power sub-cycles. The result indicated a cooling rate of 6.8 kW at a water temperature of 15^{O}C. Similarly, (Lopez-Villada et al. 2014) presented solar-based adsorption power-cooling GOC for different blends of NH_3/H_2O, $NH_3/LiNO_3$ and NH_3/NaSCN. In the power-cooling cycle using NH_3-H_2O, the monthly efficiency fluctuated between 30 and 50 %, with an annual average cooling rate not greater than 25 MWh.

3. Study contribution and novelty

However, from the surveyed literature, one key disadvantage of the studied cycles is the low cooling production rate and long pathway of working fluids to the end state for conversion. In addition, to contract this gap, the current study proposed a novel bottoming NH3-H_2O vapour-absorption system (VAS) powered by the refrigerant condensate from the vapour compression cycle (VCP) to obtain double refrigerating effect using the same working fluid. In this case, the utilization potential of the ammonia vapour exiting the VAS generator is first condensed, throttled and allowed to evaporate in the evaporator 1 (EVP1), producing cooling. The evaporated vapour from EVP 1 is compressed in the VCP system to increase the kinetic energy and further re-condensed, re-throttled and allowed to evaporate in EVP 2, thus producing an equivalent refrigerating effect in the VAS. The topping cycle, ORC powered by solar energy, produces power, heating and hot water supply. Additionally, the conceived configuration is uncommon in literature,

and the author has considered it noteworthy. However, the mathematical simulation, the thermodynamic analysis and the sustainability are performed to estimate the practicability of the proposed system.

4. Methodology

In simulating the mathematical models describing the proposed power-cooling system, the models are first established and built on thermodynamics' mass and conservation principles, momentum, and energy laws with the assumptions contained in (Higa et al. 2018). The developed system will be simulated at variable operating conditions, with a code program written on EES (Engineering Equation Solver) simulator software. The NH_3-H_2O mix properties in the VAS are attainable in the EES data assemblage and integrated into the simulation platform. The input or operating parameters are presented in Table 1(Abam et al. 2020; López-Villada et al. 2014). The mathematical models for the thermodynamic performance breakdown, the energy, mass conservation and the principles of momentum are successively applied to each system component of the combined cycle as presented in the subsequent sections.

Table 1. System input operating parameters

Parameters	Value	Unit
Ambient temperature	298	K
Ambient pressure	1.013	bar
Receiver temperature	371	K
Receiver inner diameter	0.06	m
Receiver outer diameter	0.08	m
Transmittance of the glass cover	0.96	-
Absorbance of the receiver	0.96	-
Number of parallel collector rows (col_p)	3	-
Number of collectors in series (col_s)	15	-
Turbine isentropic efficiency	85	%
Pump isentropic efficiency	80	%
Turbine inlet pressure	25	bar
Turbine inlet temperature	423	K
Condenser inlet pressure	25	bar
VAS mass flow rate	7.065	kg/s
Pinch point temperature	35	K
ORC refrigerant mass flow rate	1.5	Kg/s
ORC TIP	25	Bar
ORC TIT	133.5	^oC
VAS generator pressure	4.7	Bar
VAS generator temp.	48	^oC
VAS ref. mass	0.5	Kg/s
VAS condenser pressure	1.7	Bar
VAS ammonia concentration	0.47	-
Parabolic collector heat input	351	kW

Figure 1 shows the proposed renewable energy system comprising an ORC sub-system powered by solar Energy, a water heater, and a bi-evaporator refrigeration unit. The primary energy input to the system is from a solar collector, exchanging heat through a vapour generator for driving the ORC and further heating a domestic water heater for steam generation for driving the vapour absorption system (VAS) for refrigeration. In the vapour absorption system, the generator heats the ammonium water solution to the required generator temperature, freeing a rich ammonia vapour and allowing it to condense in condenser 2, throttled and evaporate in EVP1 to produce cooling. The vapour from EVP1 is compressed and condensed in condenser 3. The condensate is throttled and allowed to evaporate in EVP 2 on the VAS side, thus producing an equivalent cooling effect. The absorber receives this stream and mixes with the

weak ammonium water solution. Water is provided in the absorber, thus forming a rich aqua ammonia solution and pumped through a heat exchanger to the generator to start the cycle.

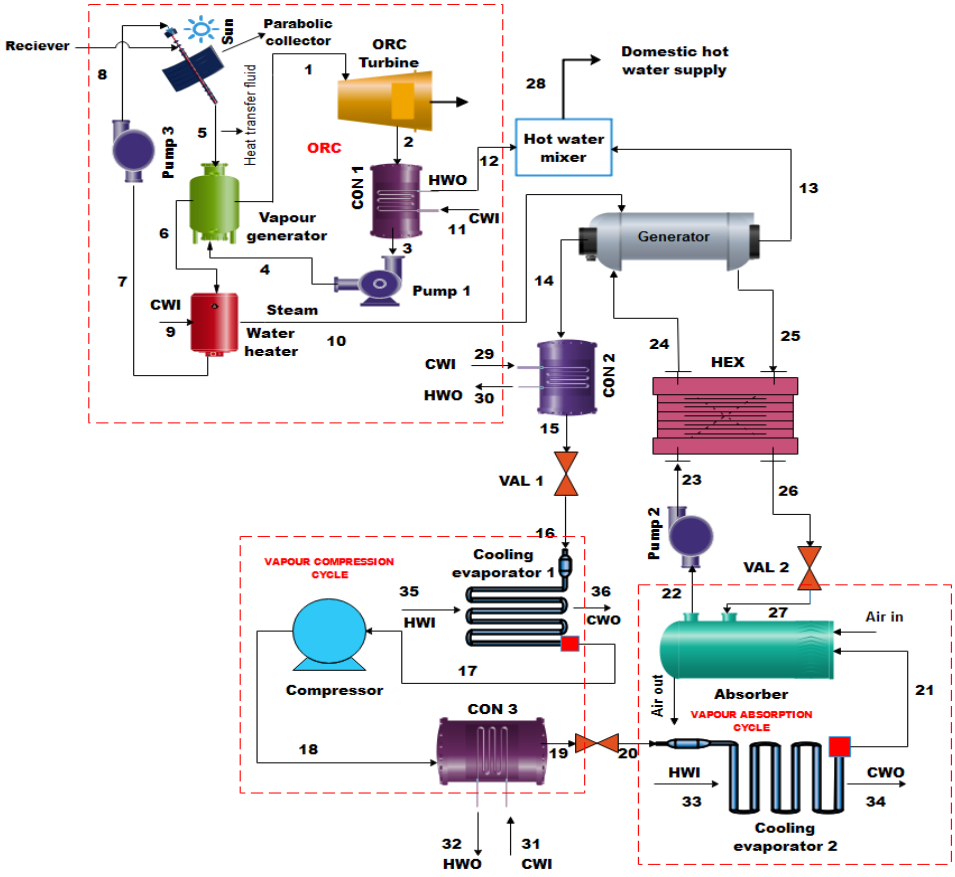

Figure 1. Schematic of the new integrated solar power-cooling ammonia–water cycle**.**

The general energy flow balance for a thermodynamic system under steady for the k^{th} component is obtained in (Ozlu and Dincer, 2015)

$$\sum \dot{Q}_k + \sum \dot{m}_i \left(h_1 + \frac{C_i^2}{2} + gz_1\right) = \sum \dot{m}_e \left(h_e + \frac{C_0^2}{2} + gz_2\right) + \sum W$$

The useful energy delivered from the parabolic solar collector (PSC) and the thermal efficiency is given as:

$$Q_u = \dot{m}_8 Cp_8 (T_8 - T_5)$$

$$Q_u = F_R[G_B \eta_0 A_a - A_r U_L (T_8 - T_{amb})]$$

$$\eta_c = \frac{Q_u}{A_a G_B}$$

The energy balance around the ORC and water heater (WHT) and the ORC thermal efficiency are expressed.

$$\dot{Q}_{VG} = \dot{m}_5 (h_5 - h_6), \ \dot{m}_5 = \dot{m}_6 \text{ and } \dot{m}_1 = \dot{m}_4$$

$$\dot{m}_6 h_6 + \dot{m}_9 h_9 = \dot{m}_7 h_7 + \dot{m}_{10} h_{10}$$

$$\eta_{ef} = \frac{\dot{W}_{ORC,tubine} - \dot{W}_{ORC,pump}}{Q_{in}}$$

The vapour absorption generator (VAG) heat input, EVP$_2$ rate and COP_{VAS} are presented

$$\dot{Q}_{VAG} = \dot{m}_{13}(h_{13} - h_{10})$$

$$\dot{Q}_{EVP2} = \dot{m}_{21}(h_{21} - h_{20})$$

$$COP_{VAS} = \frac{Q_{EVP2}}{\dot{m}_{17}(h_{18} - h_{17})}$$

Where $\dot{m}_{17}(h_{18} - h_{17})$ represent the work done by the compressor $\dot{W}_{comp}$ which drives the cooling process on the VAS side.

Similarly, the energy balance around the VCP side is shown.

$$\dot{W}_{comp} = \dot{m}_{17}(h_{18} - h_{17})$$

$$\dot{Q}_{EVP\,1} = \dot{m}_{16}(h_{17} - h_{16})$$

$$COP_{VCP} = \frac{Q_{EVP1}}{\dot{m}_{13}(h_{13} - h_{10})}$$

Where $\dot{m}_{13}(h_{13} - h_{10})$ is the energy input for the $\dot{Q}_{gen}$

The general exergy balance for a control volume in a steady state, neglecting potential, kinetic and electrical energy, is defined as in (Abam et al., 2020; Ozlu and Dincer, 2015)

$$\dot{E}_{xd} = \sum_k \left(1 - \frac{T_0}{T_k}\right)\dot{Q}_k - \dot{W}_{cv} + \sum_i \left(n_i \dot{E}x_i\right) - \sum_e \left(n_e \dot{E}x_e\right)$$

$$\dot{E}_{xD,k} = \dot{E}_{xF,k} - \dot{E}_{xPk} - \dot{E}_{xL,k}$$

The exergy efficiency,ψ_k, and the exergy destruction ratio is equally defined for the ***kth*** component as:

$$\psi_k = \frac{\dot{E}_{xPk}}{\dot{E}x_{F,k}}$$

$$Y_{D,k} = \frac{\dot{E}_{xD,k}}{\dot{E}_{xF,total}}$$

The exergetic sustainability indicators are derived for Fig. 1 following the derivation in (Abam et al. 2022) and presented in Table 2.

Table 2. Exergetic sustainability indicators (ESI) and their derivation

S/N	Exergetic sustainability indicators (ESI)	Derivation of ESI
1	Waste exergy ratio (WER) =Total exergy useful output/Total exergy input	$\frac{\dot{E}_5 + \dot{E}D_{Total}}{\dot{E}_5 - \dot{E}_6}$ (Range from 0 to 1)
2	Environmental effect factor (EEF) = Waste exergy ratio/Exergy efficiency	$\frac{\dot{E}_5 + \dot{E}D_{Total}}{W_T + \dot{E}_{,evp1} + \dot{E}_{,evp2}}$ (Range from 0 to ∞)
3	Exergy destruction ratio (EDR) = Total exergy destruction / Total exergy input	$\frac{\dot{E}D_{Total}}{\dot{E}_1 - \dot{E}_2}$ (Range from 0 to 1)

4	Exergetic sustainability index (ESI) = Total exergy of useful output /Total waste exergy output	$\frac{W_T+\dot{E}_{,evp1}+\dot{E}_{,evp2}}{\dot{E}_{13}+\dot{ED}_{Total}}$	(Range from 0 to ∞)

5. Model validation

The results of the current study are validated and compared with the study of (Abam et al. 2022) and (Higa et al.2018), as shown in Table 3. The validation was based on the following common conditions: working fluid R245fa, ORC turbine inlet temperature at 433 K, turbine inlet pressure (TIP) at 25 bar and turbine mass flow rate at 0.5772 kg/s. The variants in percentage change were calculated at 2.73% for energy efficiency and 1.59 % for exergy efficiency when compared with (Higa et al.2018). Conversely, an improvement in output power was approximated at 7.92 % and 36.28% when compared with (Higa et al. 2018) and (Abam et al. 2022), respectively. The bottoming VAS was matched with the study of (Rostamzadeh et al. 2017) (Table 3) at generator temperature and pressure of 327 K and 4.5 bar. The COP and the refrigerating effect for the present study showed a double performance enhancement despite the same input parameters. The enhancement is ascribed to the modification in the thermodynamic processes in the SORCAS model.

Table 3. System validation of the SORCAS

Parameters	(Abam et al. 2022)	(Higa et al.2018),	(Rostamzadeh et al. 2017)	Current study
ORC Turbine output (kW)	15.64	24.54	-	26.65
ORC TIT (K)	433	433	-	433
Energy efficiency (%)	14.47	37.57	-	38.63
Exergy efficiency (%)	35.47	41.46	-	42.09
Working fluid	-	-	NH_3-H_2O	NH_3-H_2O
COP (VAS)	-	-	0.256	0.643
Evaporator cooling rate (EVP1) kW	-	-	342.9	679.1
Evaporator cooling rate (EVP2) KW	-	-	926.2	679.1
Total evaporator cooling rate (kW)	-	-	1269	1358

6. Results and Discussion

The thermodynamic performance based on the operating conditions in Table 1 is presented. The results indicated a total output power of 29.65 kW from the topping ORC at collector heat input and thermal efficiency of 351 kW and 80 %, respectively. The efficiencies obtained for the ORC stood at 21.44 % for energy and 45 % for exergy. The total energy and exergy efficiencies, including the bottoming cycles, were 36.75 % and 42 %, respectively. The COP for the VCP was 1.77, whereas that for the VAS cycle was calculated at 0.66. Also, the Energy and exergy of cooling were estimated at 1355 kW and 225.8 kW at a generator input of 96.59 kW. Culminating in the refrigerating capacity of approximately 679 kW for both VCP and the VAS.

The total COP was not greater than 1.844, with about 20% enhancement from the results obtained by (Rostamzadeh et al. 2017). The performance disparities were examined with key thermodynamic parameters (i.e., the turbine inlet temperature (TIT), VAS generator pressure, and mass flow rate of heat transfer fluid). The TIT can influence the general system performance, as shown in Figure.2. The condition of the exit fluid at the turbine depends on the TIT, which defines the condition of the fluid supplied to the ORC vapour generator via hot water to the VAS generator. The TIT ranged between 388 and 415K. Between these ranges, the energy efficiency increased from 6.2 to 40 %. In contrast, exergy efficiency improved from 29.02 to approximately 55 % at a constant mass flow rate. The results indicate that for every one-degree increase in TIT, the energy efficiency increases by 0.3 %, whereas the exergy efficiency rises by about 0.41%. It can also be observed that the exergy efficiency values are higher than the energy efficiency. The reason for the phenomenon is depicted in Figure 3. As the TIT increases, the total exergy input decreases with an increase in the turbine output (TOP). For a fixed TOP, $Q_{input,total} > Ex_{input\ total}$. Thus resulting in high exergy efficiency.

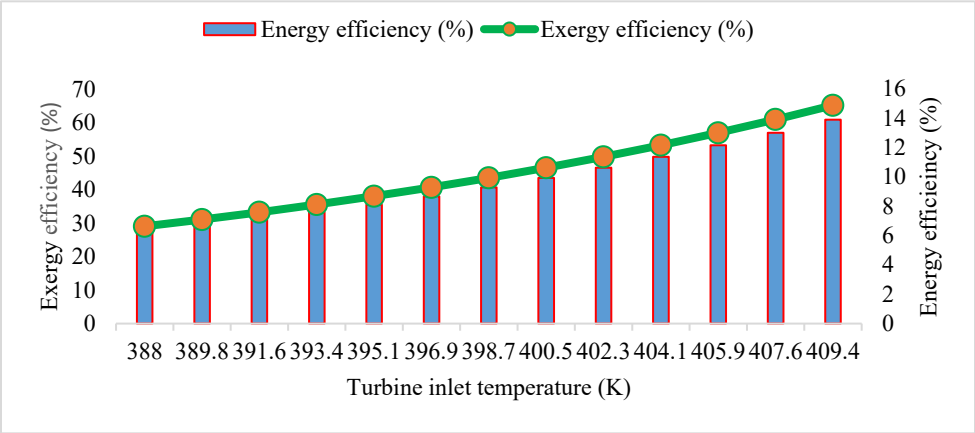

Figure 2. Turbine inlet temperature (TIT) on energy and exergy efficiencies

The effect of heat transfer fluid ($\dot{m}_5$) from the receiver of the parabolic collector was studied (Fig. 4) on the overall energy and exergy efficiencies.

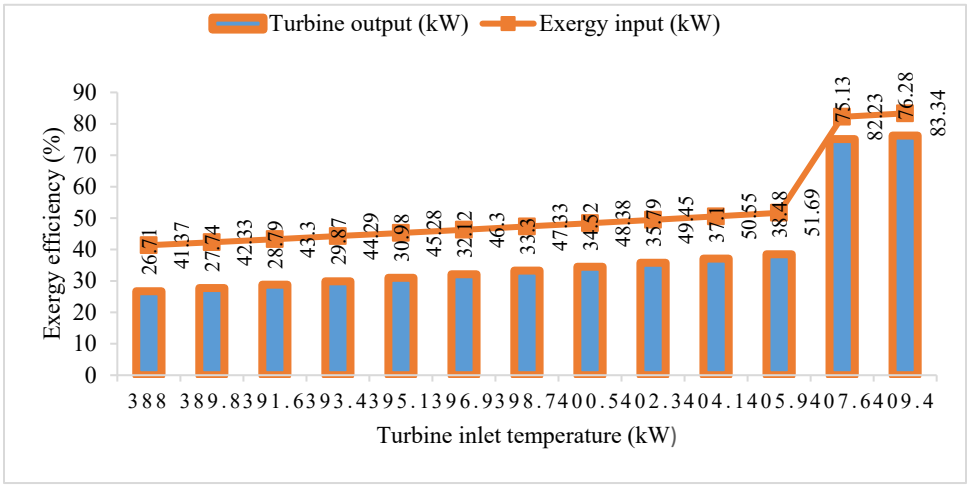

Figure 3. Turbine inlet temperature (TIT) on turbine output and exergy input

The $\dot{m}_5$ was varied between $2.103 \leq \dot{m}_5 \leq 4.341 kg/s$. Within this range, the energy and exergy efficiencies improved by 61.05 % and 61.062 %, respectively. The effects of $\dot{m}_5$ The efficiency of the plant was trifling as the efficiency gap was not more than 0.012. The small enthalpy changes with a high mass flow rate were responsible for this increment.

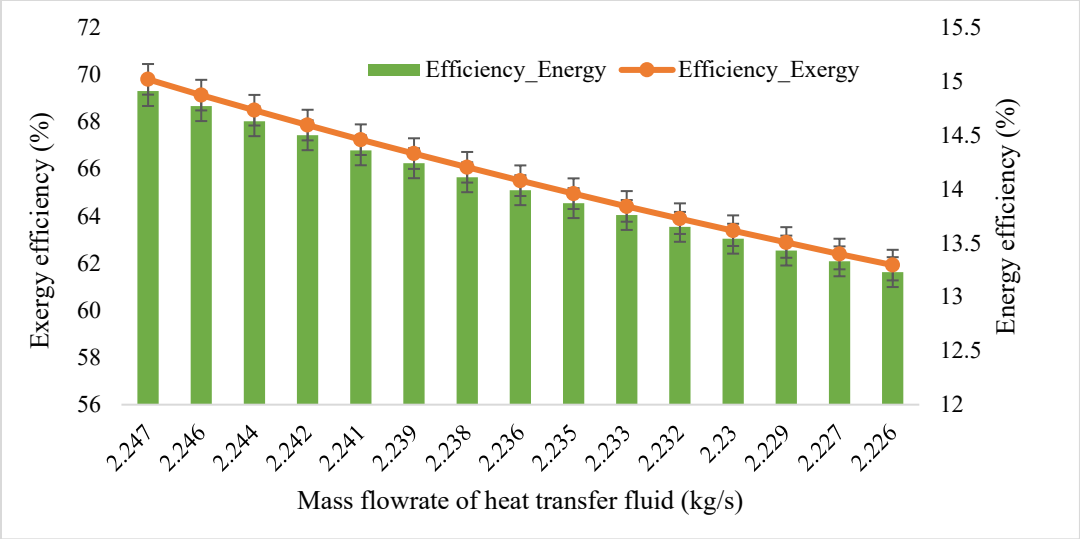

Figure 4. Effect of ($\dot{m}_5$) on energy and exergy efficiencies

The generator temperature variations on the coefficient of performance (COP) are shown in Fig.5. The overall COP increased from 1.943 at 388 K to 5.2 at 404 K. The study has achieved an equivalent refrigerating capacity for the VCP and VAS. The latter has resulted in an overall increase in COP total. However, it implies that as the generator temperature increases at a constant mass flowrate, a slight enthalpy difference exiting at the inlet and outlet of the generator results in a decrease in $Q_{generator}$. This led to an increase in $\frac{Q_{EVP1}}{Q_{generator}}$, the COP of the VCP side. Similarly, since the same condensate mass flow rate from the VCP is throttled at a very minimum temperature change, the enthalpy variation remains insignificant, thus maintaining the same refrigerating effect in the VAS as the ratio. $\frac{Q_{EVP2}}{\dot{W}_{comp}}$ increases due to the decrease in the compressor work ($\dot{W}_{comp.}$).

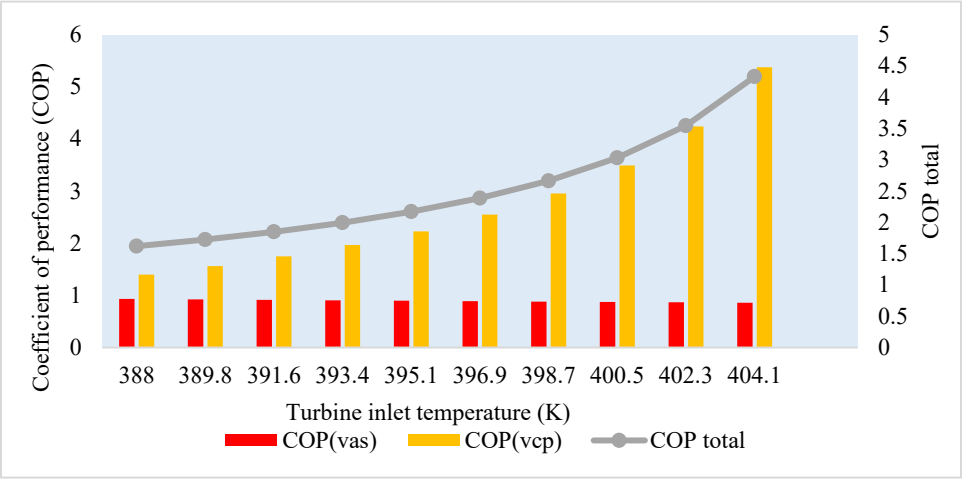

Figure 5. Generator temperature effect on COP

The effect of the VAS generator pressure on the energetic sustainability indicators such as waste exergy ratio (WER), environmental effect factor (EEF), exergy destruction ratio (EDR) and energetic sustainability index (ESI) is presented in (Figure. 6). The generator pressure was considered between 4.75 bar and 4.90 bar.

The results show that increasing generator pressure decreases sustainability values or indicators. The EEF decreased from 1.35 to 1.12 between the generator pressures (P_{gen}) of $4.75 \leq P_{gen} \leq 4.90\ bar$. At the same pressure range, the ESI increased from 1.77 to 1.82, equivalent to 2.75 %. However, the values of WER. The reason for the improvement in the sustainability indicator is the decrease in the exergy destruction across the increase in pressure. Another factor that enhances the system's sustainability is the type of fluid, operating parameters, system configuration, and the reduction in the thermodynamic pathways to the end state.

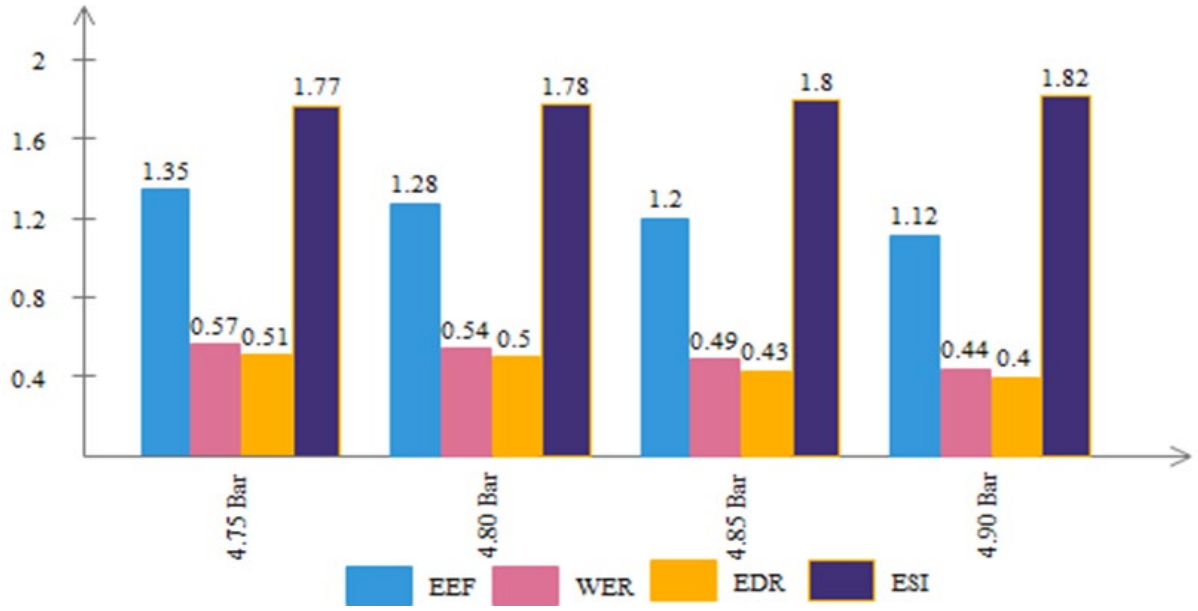

Figure 6. Effect of generator pressure on energetic sustainability indicator

7. Conclusion

The thermodynamic and sustainability analysis of a novel solar-powered ORC system integrated with single-effect absorption-VCP refrigeration cycles for domestic electricity/cooling supply was performed in this study. Furthermore, to demonstrate the system's viability, a parametric study was conducted to observe certain thermodynamic variations. The overall efficiencies, energy and exergy, were estimated at 36.75 % for Energy and 42 % for exergy. The system's overall cooling rate was 3259 kW with a maximum COP of 3.046. The increase in COP is attributed to the reduction in the generator heat rate, which decreases as the pressure increases. The COP of the system was found to increase at a higher generator pressure. The maximum ESI of 1.82 was obtained while the EEF fluctuated between 1.35 and 1.12 at generator pressure of 4.75 and 4.90 bar. The results indicated an increase in ESI for increasing generator pressure. The WER show a decreasing trend, indicating that the proposed system has high sustainability.

References

Abam, F.I., Diemuodeke, O.E., Ekwe, E.B., Alghassab, M., Samuel, O.D., Khan, Z.A., Imran, M., Farooq, M. Exergoeconomic and Environmental Modeling of Integrated Polygeneration Power Plant with Biomass-Based Syngas Supplemental Firing, *Energies* 13, 6018, 2020.

Abam, F.I., Inah, O.I., Effiom, S.O., Ntunde, D.I., Ugwu, H.U., Ndukwu, M.C., and Samuel, O.D. Projection of sustainability indicators, emissions and improvement potential of the energy drivers in the Nigerian transport sector based on exergy procedure, Scientific African 16, e01175, 2022.

Abam, F.I., Okon, B.B., Ekwe, E. B., Isaac, J., Effiom, S. O., Ndukwu, M. C., Inah, O.I., Ubi, P.A., Oyedepo, S., Ohunakin, O. S. Thermoeconomic and exergoenvironmental sustainability of a power-cooling organic Rankine cycle with ejector system, *E-Prime Advances in Electrical Engineering, Electronics and Energy,* 2, 100064, 2022.

Ayou DS., Eveloy, V. Energy, exergy and exergoeconomic analysis of an ultra low-grade heat- driven ammonia-water combined absorption power-cooling cycle for district space cooling, sub-zero refrigeration, power and LNG regasification. Energy Conversion Management 213, 112790, 2020.

Goswami, D.Y. Solar thermal power technology: present status and ideas for the future, Energy Sources. 20, 137-145, 1998.
Goswami, D.Y. Solar thermal power: status of technologies and opportunities for research, *Heat and Mass Transfer*, 95, 57–60, 1995.
Goswami, D.Y., and Xu, F. Analysis of a new thermodynamic cycle for combined power and cooling using low and mid temperature solar collectors, Journal of Solar Energy Engineering, 121, 91–97, 1999.
Han, W., Chen, Q., Sun, L., Ma, S., Zhao, T., Zheng, D., and Jin, H. Experimental studies on a combined refrigeration/power generation system activated by low-grade heat, *Energy*, 74, 59-66, 2014.
Higa, M., Yamamoto, E.Y., Oliveira, J.C.D. de., Conceição, W.A.S. Evaluation of the integration of an ammonia-water power cycle in an absorption refrigeration system of an industrial plant, *Energy Conversion Management,* 178, 265-276, 2018.
Jing, X., and Zheng, D. Effect of cycle coupling-configuration on energy cascade utilization for a new power and cooling cogeneration cycle, Energy Conversion Management,78, 58-64, 2014.
Kim, K.H. Thermal analysis of a combined absorption cycle of cogeneration of power and cooling for use of low temperature source, *Korean Journal of Air-Conditioning and Refrigeration Engineering*, 23, 413–420, 2011.
López-Villada, J., Ayou, D.S. Bruno, J.C., Coronas, A. Modelling, simulation and analysis of solar absorption power-cooling systems, International Journal of Refrigeration. 39, 125–136, 2014.
Mendoza, L.C., Ayou, D.S., Navarro-Esbrí J., Bruno, J.C. Coronas, A. Small capacity absorption systems for cooling and power with a scroll expander and ammonia based working fluids, Appl Therm Eng. 72 (2014) 258–265. https://doi.org/10.1016/j.applthermaleng.2014.06.019.
Ozlu, S., and Dincer, I. Development and analysis of a solar and wind energy based multigeneration system, *Solar Energy*. 122, 1279-1295, 2015.
Padilla, R.V., Demirkaya, G., Goswami, D.Y., Stefanakos, E., and Rahman, M.M. Analysis of power and cooling cogeneration using ammonia-water mixture, *Energy*, 35, 4649- 4657, 2010.
Rostamzadeh, H., Ebadollahi, M., Ghaebi, H., Amidpour, M., Kheiri, R. Energy and exergy analysis of novel combined cooling and power (CCP) cycles, Applied Thermal Engineering, 124, 152-169, 2017.
Sun, L., Han, W., Jing, X., Zheng, D., Jin, H. A power and cooling cogeneration system using mid/low-temperature heat source, Appl Energy, 112, 886-897, 2013.
Wang, J., Wang, J., Zhao., and Dai, Y. Thermodynamic analysis of a new combined cooling and power system using ammonia–water mixture, *Energy Conversion and Management*, 117, 335-342, 2016.
Xu, F., Goswami, D.Y., and Bhagwat, S.S. A combined power/cooling cycle, *Energy,* 25, 233-246, 2000.
Yu, Z., Han, J., Liu, H., and Zhao, H. Theoretical study on a novel ammonia–water cogeneration system with adjustable cooling to power ratios, *Applied Energy* 122, 53-61, 2014.

Biographies

Fidelis I. Abam received his M.Sc and PhD degrees in Mechanical Engineering with specifics in Energy and Power Engineering from the University of Lagos in 2008 and the University of Nigeria Nsukka in 2011. He is currently a Research Professor at the University of Calabar, Nigeria. **Professor Abam** has shown scholarly distinction over time. Having ranked among the top 500 researchers in Nigeria by Scholarly domain from 2019 to date. Regarding national research contributions, Professor Abam was the pioneering research fellow and the residential sector lead for Nigeria's Deep Decarbonization Pathways (DDP) project. The project objective was the mobilization and reinforcement of the capacities of local teams of experts and researchers for the scientific analysis of low-emission development pathways in Nigeria. Currently, he is actively involved in research in renewable energy system modelling, energy conversion and generation, energy efficiency, and environmental sustainability, with specifics in low-grade energy conversion technologies and multigeneration energy systems.

Bassey B. Okon holds a PhD in Mechanical Engineering from the University of Manchester in the United Kingdom in 2013. He is an Associate Professor in the Department of Mechanical Engineering at the Federal University of Technology Ikot Abasi, Akwa Ibom State, Nigeria. Currently, he is a Commissioner in the Akwa Ibom State Government of Nigeria, where he oversees the design and development of the Ibom Sea Port.

Isuamfon Edem Is a Researcher and the current Head of the Department of Mechanical Engineering at Akwa Ibom State University (AKSU), Ikot Akpaden, Akwa Ibom State, Nigeria. He obtained his Bachelor of Science and Master

of Science degrees in Mechanical Engineering at the Peoples' Friendship University of Russia (RUDN), Moscow, Russia, in 2007 and 2009 respectively. He obtained a PhD in Mechanical Engineering specializing in Energy modelling of machine tool axis and toolpaths at the University of Manchester, United Kingdom, in 2016. His research interests include Energy efficiency in machining, Sustainable manufacturing, CNC machining, and Green manufacturing.

NOMENCLATURE

A_a	aperture area (m^2)
COP	Coefficient of performance
$\dot{E}_D$	exergy destruction (kW)
$\dot{E}_x$	exergy flow rate (kW)
F_R	Heat removal factor
h	specific enthalpy, kJ/kg
$\dot{m}$	mass flow rate (kg/s)
P	pressure (kPa)
$\dot{Q}$	heat transfer rate (kW)
T	temperature, K
U_0	overall heat transfer coefficient (W/m^2K)
$\dot{W}$	work transfer rate (kW)

Abbreviations

EVP	evaporator
ORC	organic Rankine cycle
ORCVG	ORC vapour generator
ORC TIT	ORC turbine inlet temperature
VCP	vapour compression
VAG	vapour generator
VAS	vapour absorption system

Subscripts

i, j	inlet and exit
k	plant component

Greek symbol

η_{ex}	energy efficiency (%)
ψ	exergy efficiency (%)